Lotus-Shaped Negative Curvature Hollow Core Fiber With 10.5 dB/km at 1550 nm Wavelength

Mubassira Banu Syed Nawazuddin (iD), *Member, IEEE*, Natalie V. Wheeler, John R. Hayes (iD), *Member, OSA*, Seyed Reza Sandoghchi (iD), *Member, IEEE, Member, OSA*, Thomas D. Bradley, *Member, OSA*, Gregory T. Jasion, *Member, IEEE*, Radan Slavík, *Senior Member, IEEE, Fellow, OSA*, David J. Richardson (iD), *Fellow, IEEE, Fellow, OSA*, and Francesco Poletti, *Member, IEEE*

(Highly-Scored Paper)

Abstract—We present a novel lotus-shaped negative curvature antiresonant hollow core fiber with the potential for low loss and very wide bandwidth. A minimum loss of ∼10 dB/km at 1550 nm and less than 100 dB/km over a bandwidth of ∼650 nm is demonstrated, with effectively single mode behavior over lengths of a few tens of meters. We demonstrate power penalty free 10.5-Gb/s data transmission through an 86 m length of fiber at both O and C telecom bands. The fiber macrobend sensitivity has also been tested, which is relevant for telecom as well as for other applications including beam delivery and gas-based sensing. The bend loss is found to be below 0.2 dB/m for bend radii down to 8 cm at wavelengths away from the short wavelength edge of the transmission band.

Index Terms—Fiber optics communications, hollow core optical fibers, low latency, microstructured optical fibers.

I. INTRODUCTION

DUE to the unique guidance mechanisms offered by hollow core photonic crystal fibers (HC-PCFs), which enable light transmission in low index media such as air and vacuum, these fibers are great contenders for applications in low latency data communications [1], [2]. Furthermore, they also have potential use in gas based linear/non-linear optics, laser and particle guidance and high power, ultra-short pulse delivery [3], [4]. Based on their guidance mechanism, HC-PCFs are broadly categorised as hollow core photonic bandgap fibers (HC-PBGFs) and hollow core antiresonant/inhibited coupling fibers (HC-ARF). Within the broad HC-ARF category, many different fiber topologies have emerged, such as those with a Kagome cladding (K-HCF) [5]–[7], or a simpler structure with a single ring of touching or non-touching/non-contact tubes as antiresonant elements [8]–[12].
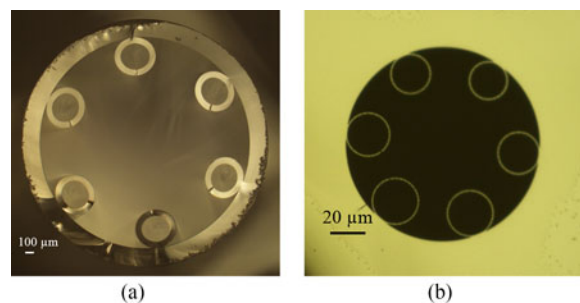
Fig. 1. (a) Microscope image of a cane, (b) Microscope image of a fabricated typical single ring NCTHC-ARF.

To date, HC-PBGFs still offer the lowest loss recorded for HC-PCFs, although this comes at the expense of useable bandwidth, only 10 s of nm in the lowest loss fiber [13]. While this can be extended to up to ∼200 nm, this yields some compromise on the minimum loss [2]. On the other hand, in recent years the loss in K-HCFs, which offer octave wide bandwidth, has improved so much that at certain wavelengths they can already compete with HC-PBGFs, albeit with an increased bend loss [6], [7]. The main reason behind such dramatic recent improvement has been the realization of the importance of imposing a negative curvature hollow core boundary [5], [8] and [10]–[12].

Early works observed that a K-HCF with a negative curvature core wall significantly reduced attenuation as compared to the standard core geometry [5]. These fibers were soon followed by attempts to reduce the cladding complexity by using a single ring of non-contacting tubes (NCT) surrounding the core. This was found to allow not only a faster preform preparation compared to HC-PBGFs or K-HCFs, but also in certain cases a lower transmission loss and a wider bandwidth [9], [12]. However, one of the main practical challenges in the fabrication of such non-contact tubular hollow core ARFs (henceforth referred to as NCTHC-ARF) is to achieve the required high structural uniformity in: (i) the gap between the non-contact tubular elements and (ii) the size (and by mass conservation the thickness) of each glass tube. To illustrate the typical non-uniformities that can be observed in these fibers, we show in Fig. 1 an example of a single ring NCTHC-ARF fabricated in our group. While this is only one example, all NCTHC-ARFs reported to date
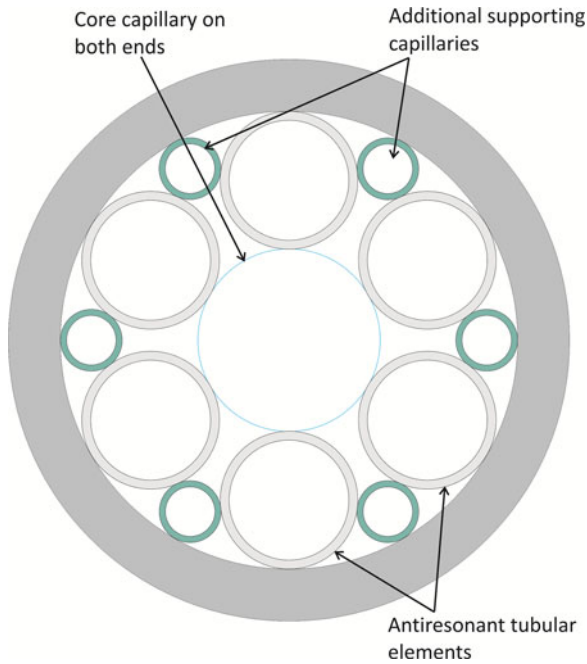
Fig. 2.   Schematic drawing showing the cross section of the stack design.
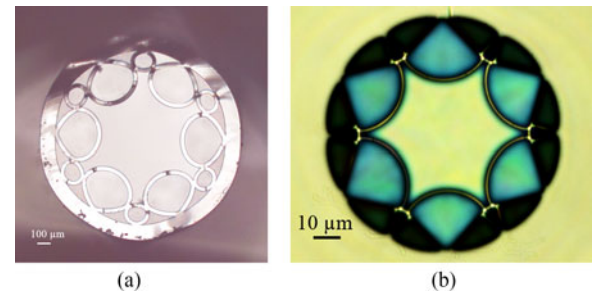

Fig. 3.   Microscope image showing cross sections of the fabricated: (a) cane and (b) Lotus NCTHC-ARF.
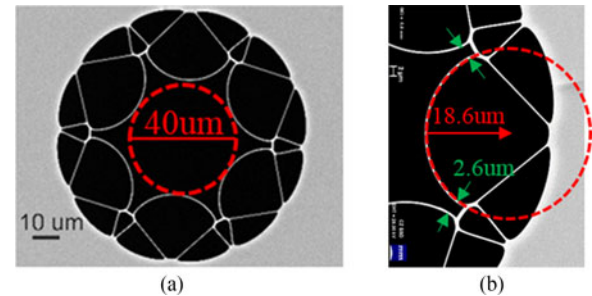

Fig. 4.   Electron micrograph of the full fiber cross section showing (a) core diameter, (b) antiresonant tubular element dimension and inter-tube gap.

seem to qualitatively present these undesirable features [8], [9] and [11].

The optical microscope image of the cane (or primary preform) is shown in Fig. 1(a). From this image, the cane structure appears symmetric. Yet, fiber fabricated from this cane [see Fig. 1(b)] has non-uniform gaps between the tubular elements; this prevents narrow gaps between the elements being achieved without some of the tubes contacting each other. Pressurisation during the fiber draw accentuates any small initial differences between the tubes that may be present in the cane. In this case, this introduces 10–20% differences in the size of all the tubular elements. The increased gap between the tubes increases the leakage loss in such fibers, while any difference in the wall thicknesses of the single ring tubular elements will contribute to wider resonance peaks, which narrow the transmission bandwidth.

Here, we address these fabrication limitations by including additional smaller diameter capillaries in between the original tubes to help maintain a uniform gap between the antiresonant elements. This type of NCTHC-ARF is regarded as having a "Lotus" shaped core which is formed during the fiber drawing by the equilibrium between gas pressure in the holes and the surface tension of the fiber material. We have published some preliminary results of this work in [14].

II. FIBER DESIGN AND FABRICATION

The schematic drawing of the primary stack design is shown in Fig. 2. We chose 6 uniform capillaries with a diameter of ∼3.9 mm to make the preform which eventually form the main antiresonant tubular elements and a further 6 additional capillaries (smaller by a factor of 2) are included between the larger capillaries and the jacket tube. The core capillary shown in the center is used only at either end of the initial preform to support the stacked capillaries prior to drawing.

To fabricate the Lotus shape NCTHC-ARF, we used the standard two stage stack and draw technique. The cross section of fabricated cane and fiber are shown in Fig. 3(a) and (b) respectively. As can be seen, a small and very uniform gap between the large tubes is achieved in both the cane [see Fig. 3(a)] and the fiber [see Fig. 3(b)]. This is essential to minimise leakage loss through the gaps [15]. The critical fiber parameters such as the core radius, core wall thickness, microstructure radius and the fiber outer diameter are controlled by modifying the draw parameters. The structural dimensions of the fabricated fiber are shown in Fig. 4. The measured structural dimensions show exceptional uniformity in terms of gap between the tubes and radius of the antiresonant tubular elements. It has a core diameter of 40 μm (defined as the maximum diameter of a circle that can be inscribed inside the core), an average antiresonant tube radius of 18.6 μm (with a standard deviation of 0.27 μm) and the average tube thickness is ∼425 nm. The mean gap between the tubes is 2.6 μm (with a standard deviation of 0.07 μm). Table I shows a comparison of geometrical parameters of the Lotus NCTHC-ARF with a 7 tube NCTHC-ARF developed in our group [9].

While the additional small spacing tubes are very effective in increasing the cross-sectional uniformity of the structure, they also lead to the presence of nodes, where the big and small capillaries contact. These nodes can act as independent waveguides, introducing additional resonances in the spectrum. However, the negative curvature in the core surround wall helps to introduce a radial separation between the core modes and the high loss glass modes guided in the nodes, which significantly reduces coupling between them.

TABLE I
COMPARISON OF LOTUS SHAPED NCTHC-ARF WITH 7 TUBE NCTHC-ARF

Fiber	Mean cap. radius (μm)	Mean Inter-tube gap (μm)	Core radius (μm)	Membrane thickness (nm)
7 tube NCTHC-ARF [9]	22.9±0.84	5.4±1.1	20	359
Lotus shape NCTHC-ARF	18.6±0.27	2.6±0.07	20	425

Fig. 6. Structural schematics of three different geometries: (a) full lattice lotus structure, (b) arc only geometry and (c) extended arc geometry and their corresponding simulated mode field patterns: (d), (e) and (f).
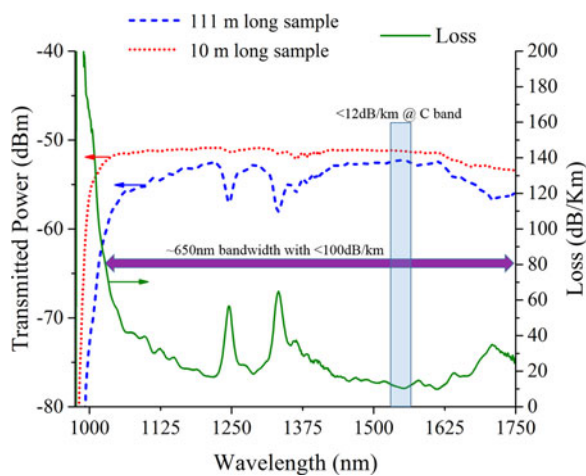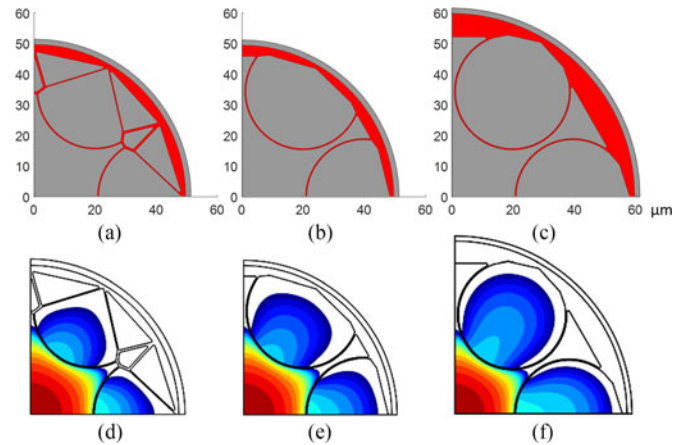

Fig. 5. Measured transmission spectra of 111 m (blue-dash) and 10 m (red-dots) cut back length with the calculated cut back loss (green).

III. FIBER CHARACTERISATION AND MODELLING

A. Attenuation

To measure the loss of the Lotus shape NCTHC-ARF, a cut-back loss measurement was carried out on a 111 m long sample. The fiber was loosely coiled on the measurement bench to a diameter of ∼30 cm. A white light source was launched into the fiber through a butt-coupled launch fiber with a closely matched mode field diameter. An optical spectrum analyser (OSA, 400–1750 nm) was used to measure the transmission spectrum. The measured transmission and loss spectra are shown in Fig. 5. The lowest loss measured is 9.8 dB/km at 1612 nm and a loss of 10.5 dB/km is observed at 1550 nm. This presents the lowest loss recorded at a wavelength of 1550 nm with a NCTHC-ARF to date. The fiber shows a wide operational bandwidth, with loss <100 dB/km over significantly more than ∼650 nm, measured with a conventional optical spectrum analyser. The measured bandwidth is not inherently limited by the fiber design but rather by the spectral response of the OSA on the long wavelength edge. Around 1245 nm and 1332 nm, two loss peaks of ∼50/70 dB/km are noticeable, which we interpret as resonance peaks caused by the nodes where the big and small tubular

elements contact. However, these do not prevent the fiber operating in the O and C telecoms bands.

B. Modelling

A theoretical study was performed to identify the effect and contribution of these struts/nodes. To identify the main structural features responsible for the low loss in the fiber, two additional geometries were modelled using Comsol. The 2D cross section of the fiber was modelled in Comsol to find the mode fields and confinement losses. The surface scattering loss is also estimated from the normalized electric field at the interfaces. The methods we followed to do these simulations are similar to those explained in detail in Ref. [15]. The structural diagrams of all three geometries along with their simulated mode field patterns are shown in Fig. 6. In all three structures, the core radius and curvature of the antiresonant elements remain the same. Fig. 6(a) shows the fabricated NCTHC-ARF having the full lattice lotus structure. The arc only geometry shown in Fig. 6(b) has core surround arcs with the same curvature as the fabricated fiber, which continue all the way to the jacket, however, it does not have the smaller tubes and the nodes associated. In the extended arc geometry [see Fig. 6(c)], the outer jacket is pushed further away to allow the arcs to continue into an almost tubular structure.

Fig. 7 shows the calculated loss (including both confinement and scattering contributions) of all three geometries, compared with the experimentally measured loss. As can be seen, the simulated loss of the full lattice lotus structure lies in a similar range to the measured loss, and the presence of some loss peaks (although not exactly at the same spectral position) is also captured by the simulations. In contrast, the calculated loss of the other two geometries having no nodes is over one order of magnitude higher. The reason for such higher loss in both nodeless geometries [see Fig. 6(b) and (c)] is that the air modes guided in the capillaries are close in effective index to the fundamental core mode, as they have very similar sizes, and thus they can easily phase match [see simulated mode field patterns
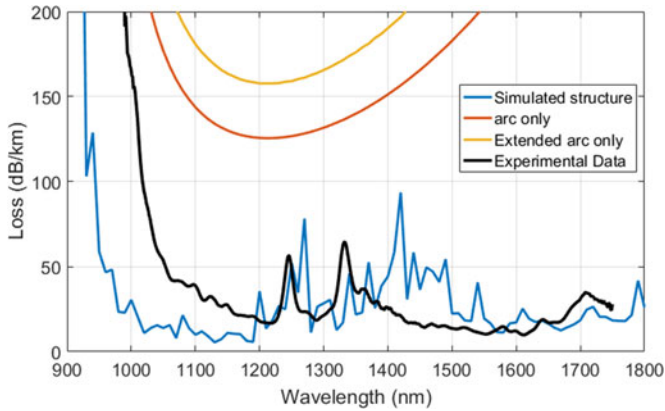
Fig. 7. Calculated loss (including both confinement and scattering contributions) of all three geometries compared with the measured cutback loss of the Lotus shaped NCTHC-ARF.

Fig. 8. Measured bend loss as a function of bend radius.

Fig. 9. Bend loss as a function of wavelength for different bend radii.

shown in Fig. 6(e) and (f)]. However in the complete lattice lotus structure the tube area is decreased by the presence of the straight elements at the back of the tubes, and these struts act as reflectors preventing the mode field from extending as far into the solid cladding [see Fig. 6(d)]. The simulations also indicate that the observed total attenuation in this fiber is dominated by confinement loss (CL). One way to reduce the dominating CL in the HC-AR fibers is to have a large core diameter. However, the large core increases the bend loss significantly. The Lotus fiber presented here has core diameter of ~40 μm, which is chosen as an optimum value to have low CL and bend loss.

The novel Lotus shaped NCTHC-ARF presented here clearly shows that the additional tubes are very effective in allowing the realisation of a uniform gap distribution and size of the tubular elements. As a consequence of this, the loss can be significantly reduced, from ~30 dB/km at telecom wavelengths in Ref. [9] to only ~10 dB/km in this work. Note that if one wanted to use a nodeless structure [both geometries 2 and 3 in Fig. 6(b) and (c)], the use of 7 or 8 tubes has been found to provide better results [8], [9], and [12].

C. Bend Loss

To understand the bend robustness in this fiber and also to explore the possibility of using this fiber for beam delivery applications, macro bend loss measurements were carried out. For this experiment, before including a bend, the transmission for the effectively straight condition is measured with an OSA. Without disturbing the input coupling and the output port, the fiber is bent on a board having different bend radii ranging from 20 cm down to 8 cm.

The length of the fiber used for this measurement is ~12 m. The bend loss as a function of radius for three different wavelengths is shown in Fig. 8. Down to bend radii of 8 cm, the attenuation due to bends for all three wavelengths does not change significantly.

The wavelength 1300 nm lies in between the two high loss resonances due to the nodes/struts, however the bend loss is not increased by their presence, as compared to wavelengths further
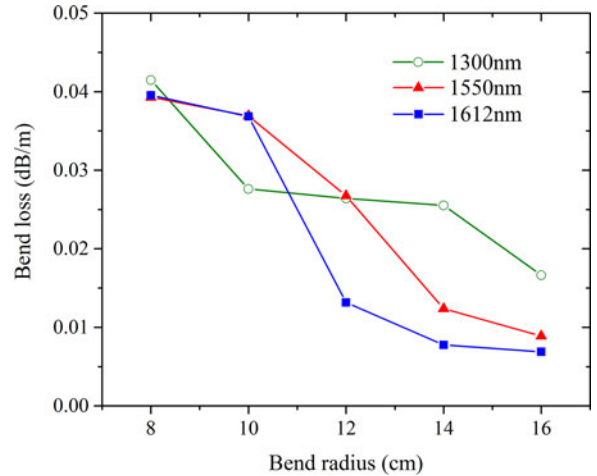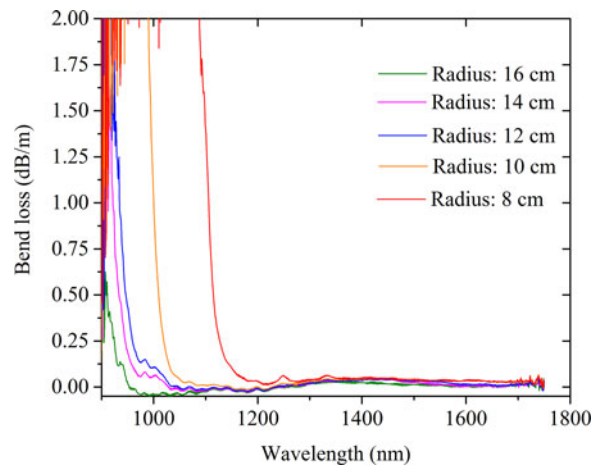
away. Besides, the resonance peaks due to the two struts/nodes are not affected by the bend. However, we notice a considerable shift of the short wavelength edge with decreasing bend radii, as shown in Fig. 9. From this and from the results in Fig. 8 one can see that at a coiled diameter of ~30 cm our cutback loss measurements at 1612 nm and 1550 nm in Fig. 5 have negligible contribution from bend loss.

D. S^2 Measurement

As in any conventional large core fiber, HC-ARFs support higher order modes (HOMs) [16], [17]. It is known, however, that a mode stripping mechanism exists that significantly attenuates most HOMs [15] in some HC-ARF designs.

To quantify the degree of HOM existence in this fiber, S^2 measurement was performed on two different lengths of fiber.

The measured results for short (23.5 m) and long (76.5 m) length samples at 1550 nm are shown in Fig. 10. The inset shows the reconstructed mode field intensity distribution of the fundamental mode and of the higher order LP_{11} mode for a short length fiber of ~23.5 m. As can be seen, there is some residual
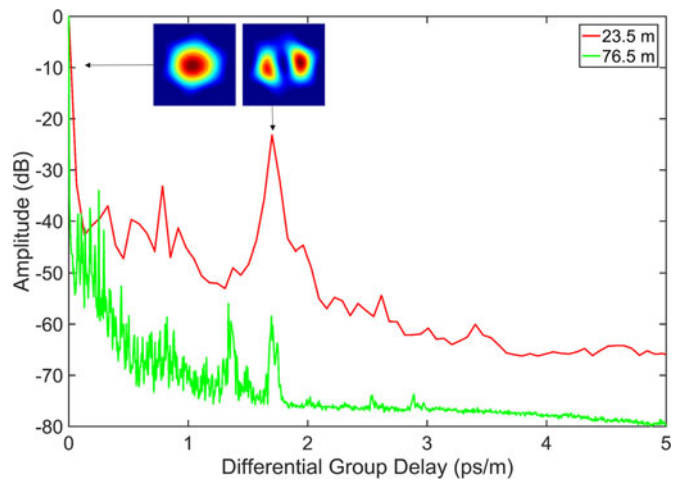
Fig. 10. Group delay curve showing the mode content of the fiber at two different lengths: 23.5 m and 76.5 m.
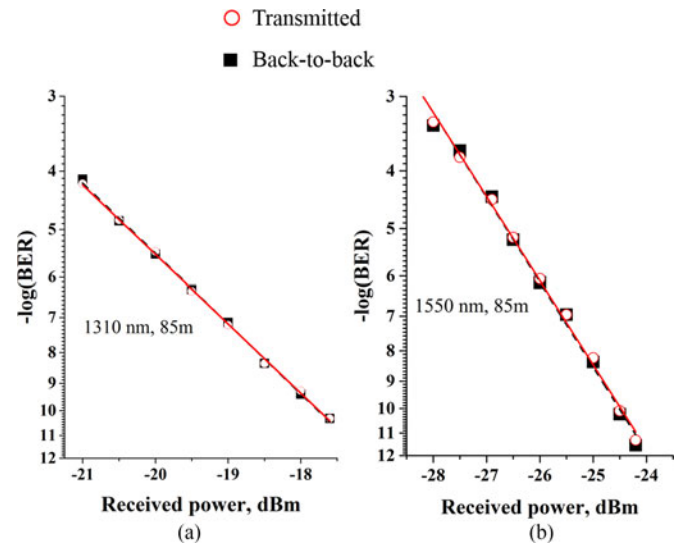

Fig. 11. BER of two different transmission wavelengths in (a) 1310 nm (O band) and (b) 1550 nm (C band). Also shown are the back-to-back measurements without any fiber.

LP_{11} mode after 23.5 m, however it becomes practically non-existent (down to about 60 dB) after 76.5 m, indicating that on long enough lengths (a few tens of metres) the fiber is essentially single mode.

IV. DATA TRANSMISSION EXPERIMENT

A 10.5-Gbit/s on-off keyed data transmission experiment was performed on the fiber to assess its potential in communications applications. We selected two wavelengths to demonstrate transmission in the two primary telecomm bands: at 1310 nm (O band) and 1550 nm (C band). The 1310 nm wavelength lies in between the two additional resonances introduced by the nodes/struts around the core, and it allows us to check whether these introduce any performance degradation. While 1550 nm is centred in the lowest loss region. To test the fiber under more challenging circumstances and study the effect that splices might have, we spliced a 10 m tail of the same fiber to the 76.5 m previously tested with S^2, using a conventional arc-fusion splicer. Due to the short lengths (and low total attenuation) involved, we were able to use a single mode fiber (SMF28) with a mode field diameter of $\sim$10 μm butt-coupled to both input and output side of the test fiber, despite the fairly large coupling loss that this caused ($\sim$14.5 dB) due to the large mode field diameter mismatch. At 1550 nm we also used a fiber pigtailed isolator to avoid any back reflection of light into the transmitter. At the receiver side the signal was analyzed with a bit error ratio (BER) tester.

Despite the additional cladding resonances near 1300 nm, the presence of a splice of the NCTHC-ARF to itself and the use of severely sub-optimal launch and collection fibers, error free (BER $< 10^{-10}$) data transmission was achieved through the full 86 m length at both wavelengths. Fig. 11 shows the resulting BER, compared with back-to-back measurements. In both instances, the BER curves show no power penalty, which is to be expected given the excellent modal properties of the fiber after such a propagation distance.

V. CONCLUSIONS

We have demonstrated a novel negative curvature hollow core antiresonant fiber with a Lotus shaped core. With additional small capillaries in the cladding structure, an exceptional structural uniformity in terms of the size of each antiresonant tubular element and the inter-tube distance is achieved. This regularity was key to produce the lowest transmission loss reported so far at 1550 nm for hollow core fibers guiding by antiresonance, of around 10 dB/km. The fiber exhibits a very wide bandwidth of well over 650 nm with $<$100 dB/km attenuation. The drawback of the presence of cladding nodes where the small stabilization tubes touch the antiresonant ones is that two resonance peaks appear in the spectrum. However, their position can be kept outside the telecoms C and L bands, and their influence on data transmission was shown to be negligible. The good modal purity and effectively single mode behavior of the fiber after a few tens of meters, measured through S^2 measurement, was exploited to transmit data. We demonstrated penalty free 10.5-Gbit/s transmission through an 86 m length of fiber (containing one splice to itself) in two different telecom bands: O and C. Bend loss measurements show low loss for bends down to 8 cm in diameter at wavelengths away from the short wavelength edge. With further loss reduction by introducing additional nested tubes within the lotus structure [15], these fibers could become serious contenders for applications such as low latency data transmission applications, for transmission of light below the silica Rayleigh scattering limit in the spectral range UV-VIS-NIR, high energy pulse laser beam delivery and gas based non-linear optics.

References

[1] F. Poletti *et al.*, "Towards high-capacity fiber-optic communications at the speed of light in vacuum," *Nature Photon.*, vol. 7, no. 4. pp. 279–284, 2013.

[2] Y. Chen *et al.*, "Multi-kilometer long, longitudinally uniform hollow core photonic bandgap fibers for broadband low latency data transmission," *J. Lightw. Technol.*, vol. 34, no. 1, pp. 104–113, Jan. 2016.

[3] F. Benabid and P. S. J. Russell, "Hollow core photonic crystal fibers: A new regime for nonlinear optics and laser-induced guidance," in *Proc. 6th Int. Conf. Transp. Opt. Netw.*, 2004, vol. 2, pp. 84–90.

[4] C. Saraceno, F. Emaury, A. Diebold, I. Graumann, M. Golling, and U. Keller, "Trends in high-power ultrafast lasers," *Proc. SPIE*, vol. 9835, 2016, Art. no. 98350X-1.

[5] Y. Y. Wang, N. V. Wheeler, F. Couny, P. J. Roberts, and F. Benabid, "Low loss broadband transmission hypocloid-core Kagome hollow core photonic crystal fiber," *Opt. Lett.*, vol. 36, no. 5, pp. 669–671, 2011.

[6] N. V. Wheeler *et al.*, "Low loss Kagome fiber in the 1 um wavelength region," in *Proc. Specialty Opt. Fibers Meeting Adv. Photon. Congr.*, 2016, Paper SoM3F.2.

[7] N. V. Wheeler *et al.*, "Low loss Kagome hollow core fibers operating from the near- to the mid-IR," *Opt. Lett.*, vol. 42, no. 13, pp. 2571–2574, 2017.

[8] A. D. Pryamikov, A. S. Biriukov, A. F. Kosolapov, V. G. Plotnichenko, S. L. Semjonov, and E. M. Dianov, "Demonstration of a waveguide regime for a silica hollow core microstructured optical fiber with a negative curvature of the core boundary in the spectral region $>3.5 \mu$m," *Opt. Express*, vol. 19, no. 2, pp. 1441–1448, 2011.

[9] J. R. Hayes *et al.*, "Antiresonant hollow core fiber with an octave spanning bandwidth for short haul data communications," *J. Lightw. Technol.*, vol. 35, no. 3, pp. 437–442, Feb. 2017.

[10] F. Yu and J. C. Knight, "Negative curvature hollow core optical fiber," *IEEE J. Sel. Topics Quantum Electron.*, vol. 22, no. 2, Mar./Apr. 2016, Art. no. 4400610.

[11] C. Wei, R. J. Weiblen, C. R. Menyuk, and J. Hu, "Negative curvature fibers," *Adv. Opt. Photon.*, vol. 9, no. 3, pp. 504–561, p. 562, 2017.

[12] B. Debord *et al.*, "Ultra low transmission loss in inhibited-coupling guiding hollow core fibers," *Optica*, vol. 4, no. 2, pp. 209–217, 2017.

[13] B. J. Mangan *et al.*, "Low loss (1.7 dB/km) hollow core photonic bandgap fiber," in *Proc. PDP Opt. Fiber Commun. Conf.*, 2004, Paper PDP24.

[14] M. B. S. Nawazuddin *et al.*, "Lotus shaped negative curvature hollow core fiber with 10.5 dB/km at 1550 nm wavelength," in *Proc. 43rd Eur. Conf. Opt. Commun.*, 2017, Paper Tu.1.A.2.

[15] F. Poletti, "Nested antiresonant nodeless hollow core fiber," *Opt. Express*, vol. 22, pp. 23807–23828, 2014.

[16] T. D. Bradley *et al.*, "Modal content in hypocycloid Kagomé hollow core photonic crystal fibers," *Opt. Express*, vol. 24, no. 14, pp. 15798–15812, 2016.

[17] V. Bock *et al.*, "Modal content measurements (S^2) of negative curvature hollow-core photonic crystal fibers," *Opt. Express*, vol. 25, no. 4, pp. 3006–3012, 2017.

Natalie V. Wheeler received the Ph.D. degree from the University of Bath, Bath, U.K., in 2011, in the fabrication and integration of hollow core photonic crystal fibers (HC-PCFs) for use as gas cells in applications including frequency metrology and slow light.

In 2010, she started as a Research Fellow with the Optoelectronics Research Centre, University of Southampton, Southampton, U.K., working on the fabrication of HC-PCFs for telecommunications applications, designing, and fabricating HC-PCFs, which have been used in world-leading transmission experiments that highlight the potential of HC-PCFs in future high-capacity transmission networks. She has coauthored more than 120 journal and conference papers. Her current research interests also include fabrication of low-loss and low-bend sensitivity HC-PCFs for operation in the mid-IR and gas spectroscopy. She is a recipient of the prestigious Royal Society University Research Fellowship.

John R. Hayes received the Ph.D. degree from the Optoelectronics Research Centre (ORC), Southampton, U.K., for the development of highly innovative microstructured fibers.

In 2003, from industry, he joined the ORC, where he was with Pirelli developing the vapor axial deposition (VAD) method for the high-volume manufacture of single-mode telecoms fibers. He was part of a team that initially transferred VAD technology from Sumitomo Electric Industries, Japan, and established a U.K. fiber manufacturing facility, and later became the Head of a team of engineers that supported its 24/7 operation. Since joining the ORC, he has created a diverse range of novel microstructured fibers and has coauthored more than 110 conference and journal papers. He is a member of the Optical Society of America.

Seyed Reza Sandoghchi (S'11–M'17) received the Bachelor's (Hons.) degree in telecommunication engineering from the Sadjad Institute of Higher Education, Mashhad, Iran, in 2005, the Master of Engineering degree in optical telecommunication from the University of Malaya, Kuala Lumpur, Malaysia, in 2011. He has been awarded the Ph.D. degree by Optoelectronics Research Centre, University of Southampton, Southampton, U.K. in 2017, and is currently working as a Research Fellow in the same institute.

He has a strong background in electromagnetism, numerical modeling, and optical fiber fabrication. His research interest includes among other microscopy and nanoscopy, and fiber characterization methods. His current research interests include hollow core photonic band gap fibers, where his main research activities include developing characterization systems.

Mubassira Banu Syed Nawazuddin (M'15) received the Bachelor of Engineering degree in electronics and communication from the University of Madras, Chennai, India, in 2004, the Master of Technology degree in electronics and instrumentation with a specialization in sensor systems technology from Vellore Institute of Technology, Vellore, India, in 2006, and the Ph.D. degree for the work titled Micromachined parallel plate structures for Casimir force measurement and Optical modulation from MESA+ Institute of Nanotechnology, University of Twente, Enschede, the Netherlands, in 2013.

After completing the Master of Technology degree, she joined, as a Research Assistant, the Microwave Laboratory, Indian Institute of Sciences, India, where she worked on the design and simulation of RF MEMS switches. In 2008, she moved to Netherlands to pursue Ph.D. Since 2016, she has been working as a Research Fellow with the Optoelectronics Research Centre, University of Southampton, Southampton, U.K. Her research interests include fabrication and characterization of novel hollow core antiresonant fibers.

Thomas D. Bradley received the M.Physics and Ph.D. degrees from the University of Bath, Bath, U.K., in 2009 and 2014, respectively.

His Ph.D. degree and earlier career research has focused on the fabrication, characterization, and loading of gas species in both antiresonant and photonic bandgap hollow core fibers. In 2014, he joined the Optoelectronics Research Centre, Southampton, U.K., where he is currently a Postdoctoral Researcher in the microstructured optical fiber groups. His current research interests include the fabrication of low-loss antiresonant hollow core fibers, development of novel characterization tools for optical fibers, and gas filling in hollow core fibers. He was the recipient of the Best Early Career Presentation Prize at the Engineering and Physical Sciences Research Council Manufacturing the Future Conference, in 2014.

Gregory T. Jasion received the M.Eng. degree in aerospace engineering and the Ph.D. degree from the University of Southampton, Southampton, U.K.

He is a Royal Academy of Engineering Research Fellow with the University of Southampton. He specializes in the field of multiphase flow with an emphasis on computational modeling. These interests brought him to the Optoelectronics Research Centre to develop fluid dynamics models to understand and improve the fabrication process of hollow microstructured optical fibers.

Radan Slavík (M'07–SM'07) received the M.Sc. and Ph.D. degrees in optics and optoelectronics from the Faculty of Mathematics and Physics, Charles University, Prague, Czech Republic, in 1996 and 2000, respectively, and the D.Sc. degree from the Academy of Sciences of the Czech Republic, Praha, Czech Republic, in 2009.

During 1995–2000 and 2004–2009, he was with the Institute of Photonics and Electronics, Czech Academy of Sciences, Prague, Czech Republic. During 2000–2003, he was with the Centre d'Optique, Photonique et Laser, Universite Laval, QC, Canada, as a Postdoctoral Research Fellow. Since 2009, he has been with the Optoelectronics Research Centre, University of Southampton, Southampton, U.K. His research interests include optical and optics-assisted signal processing. He is a Fellow of the Optical Society of America.

David J. Richardson (F'14) received the B.Sc. and Ph.D. degrees in fundamental physics from Sussex University, Brighton, U.K., in 1985 and 1989, respectively.

He joined the Optoelectronics Research Centre (ORC), Southampton University, Southampton, U.K., in 1989. He is currently a Deputy Director of the ORC with responsibility for the ORC's fiber related activities. He is a prominent figure in the international photonics community and has authored or coauthored more than 1000 conference and journal papers and produced more than 20 patents. His current research interests include among others: optical fiber communications, microstructured optical fibers, and pulsed high-power fiber lasers. He received a Royal Society University Fellowship in 1991 in recognition of his pioneering work on short-pulsed fiber lasers. He is a Fellow of the Optical Society of America and the Institute of Engineering and Technology. He became a Fellow of the Royal Academy of Engineering in 2009.

Francesco Poletti (M'05) received the Laurea degree in electronics engineering from the University of Parma, Parma, Italy, in 2000, and the Ph.D. degree from the Optoelectronics Research Centre (ORC), Southampton, U.K., in 2007.

He is currently a Professor at the ORC. He has worked for three years on optical network design with Marconi Communications and for more than ten years on the development of new generations of microstructured optical fibers with ORC. He has coauthored more than 80 journal and 200 conference publications and produced 4 patents. His research interests include the design of photonic bandgap and antiresonant fibers, the development of fiber-optic characterization techniques, and the fabrication of non-silica-based fibers and devices. He is the recipient of a Royal Society University Fellowship and a European Research Fellowship Consolidator Grant.